IJMMM International Journal of Minerals, Metallurgy and Materials 矿物冶金与材料学报（英文版）

Latest advances and progress in the microbubble flotation of fine minerals: Microbubble preparation, equipment, and applications

Ziyong Chang, Sensen Niu, Zhengchang Shen, Laichang Zou, and Huajun Wang

Cite this article as:
Ziyong Chang, Sensen Niu, Zhengchang Shen, Laichang Zou, and Huajun Wang, Latest advances and progress in the microbubble flotation of fine minerals: Microbubble preparation, equipment, and applications, *Int. J. Miner. Metall. Mater.*, 30(2023), No. 7, pp. 1244-1260. https://doi.org/10.1007/s12613-023-2615-8

View the article online at SpringerLink or IJMMM Webpage.

Articles you may be interested in

Wan-zhong Yin and Yuan Tang, Interactive effect of minerals on complex ore flotation: A brief review, *Int. J. Miner. Metall. Mater.*, 27(2020), No. 5, pp. 571-583. https://doi.org/10.1007/s12613-020-1999-y

Yong-xing Zheng, Jilai Ning, Wei Liu, Pan-jin Hu, Jin-fang Lü, and Jie Pang, Reaction behaviors of Pb and Zn sulfates during reduction roasting of Zn leaching residue and flotation of artificial sulfide minerals, *Int. J. Miner. Metall. Mater.*, 28(2021), No. 3, pp. 358-366. https://doi.org/10.1007/s12613-020-2029-9

Ataallah Bahrami, Mirsaleh Mirmohammadi, Yousef Ghorbani, Fatemeh Kazemi, Morteza Abdollahi, and Abolfazl Danesh, Process mineralogy as a key factor affecting the flotation kinetics of copper sulfide minerals, *Int. J. Miner. Metall. Mater.*, 26(2019), No. 4, pp. 430-439. https://doi.org/10.1007/s12613-019-1733-9

Ya-feng Fu, Wan-zhong Yin, Xian-shu Dong, Chuan-yao Sun, Bin Yang, Jin Yao, Hong-liang Li, Chuang Li, and Hyunjung Kim, New insights into the flotation responses of brucite and serpentine for different conditioning times: Surface dissolution behavior, *Int. J. Miner. Metall. Mater.*, 28(2021), No. 12, pp. 1898-1907. https://doi.org/10.1007/s12613-020-2158-1

Dong Li, Wan-zhong Yin, Ji-wei Xue, Jin Yao, Ya-feng Fu, and Qi Liu, Solution chemistry of carbonate minerals and its effects on the flotation of hematite with sodium oleate, *Int. J. Miner. Metall. Mater.*, 24(2017), No. 7, pp. 736-744. https://doi.org/10.1007/s12613-017-1457-7

Xi Zhang, Shun-wei Zhu, Yu-jiang Li, Yong-li Li, Qiang Guo, and Tao Qi, Purification of specularite by centrifugation instead of flotation to produce iron oxide red pigment, *Int. J. Miner. Metall. Mater.*, 28(2021), No. 1, pp. 56-65. https://doi.org/10.1007/s12613-020-2003-6

IJMMM WeChat

QQ author group

International Journal of Minerals, Metallurgy and Materials
Volume 30, Number 7, July 2023, Page 1244
https://doi.org/10.1007/s12613-023-2615-8

Invited Review

Latest advances and progress in the microbubble flotation of fine minerals: Microbubble preparation, equipment, and applications

Ziyong Chang[1,2)✉], *Sensen Niu*[1)], *Zhengchang Shen*[1,3)], *Laichang Zou*[2)], *and Huajun Wang*[1)]

1) Civil and Resource Engineering School, University of Science and Technology Beijing, Beijing 100083, China
2) State Key Laboratory of Comprehensive Utilization of Low-Grade Refractory Gold Ores, Shanghang 364200, China
3) BGRIMM Technology Group, State Key Laboratory of Mineral Processing, Beijing 100160, China
(Received: 12 November 2022; revised: 16 February 2023; accepted: 17 February 2023)

Abstract: In the past few decades, microbubble flotation has been widely studied in the separation and beneficiation of fine minerals. Compared with conventional flotation, microbubble flotation has obvious advantages, such as high grade and recovery and low consumption of flotation reagents. This work systematically reviews the latest advances and research progress in the flotation of fine mineral particles by microbubbles. In general, microbubbles have small bubble size, large specific surface area, high surface energy, and good selectivity and can also easily be attached to the surface of hydrophobic particles or large bubbles, greatly reducing the detaching probability of particles from bubbles. Microbubbles can be prepared by pressurized aeration and dissolved air, electrolysis, ultrasonic cavitation, photocatalysis, solvent exchange, temperature difference method (TDM), and Venturi tube and membrane method. Correspondingly, equipment for fine-particle flotation is categorized as microbubble release flotation machine, centrifugal flotation column, packed flotation column, and magnetic flotation machine. In practice, microbubble flotation has been widely studied in the beneficiation of ultrafine coals, metallic minerals, and nonmetallic minerals and exhibited superiority over conventional flotation machines. Mechanisms underpinning the promotion of fine-particle flotation by nanobubbles include the agglomeration of fine particles, high stability of nanobubbles in aqueous solutions, and enhancement of particle hydrophobicity and flotation dynamics.

Keywords: microbubble preparation; flotation; fine minerals; flotation equipment; bubble–particle interaction

1. Introduction

Flotation is widely used to separate valuable minerals from gangue minerals by taking advantage of the difference in their surface wettability. However, fine particles are hard to be floated because they are characterized by a large surface area, high surface energy, high surface solubility, and non-selective heterogeneous agglomeration [1]. In addition, the collision and adhesion probabilities between fine particles and air bubbles are extremely low because it is difficult to overcome the resistance of the hydration layer due to the low kinetic energy [2]. As a result, several fine mineral particles are discharged in tailings, which has been a big problem faced by plants all over the world.

In recent years, microbubble flotation exhibits great promise in improving the flotation of fine mineral particles. The advantages of microbubble flotation are low cost and easy operation because it requires the least consumption of chemicals and is affected only by the size of air bubbles [3]. Hydrodynamics study reveals that the dispersion of air bubbles in slurries can be improved by reducing the size of air bubbles, thereby promoting the collision and adhesion between air bubbles and fine mineral particles and improving the flotation performance of fine mineral particles [4]. In the past few years, microbubble flotation has been intensively studied in the flotation of fine particles and has received increasing attention from the academia and industry. Generally, air bubbles can be further categorized as microbubbles, micro–nanobubbles, and nanobubbles based on their diameter. Specifically, microbubbles are tiny bubbles with a diameter less than a few hundred microns, micro–nanobubbles are tiny bubbles with a diameter in the range of 0.1–50 μm, and nanobubble diameter ranges from 10 to 100 nm [5]. Ahmed *et al*. [6] reported that the flotation rate of fine particles is closely associated with the size of air bubbles. The flotation rate significantly increased by 100 times when the size of air bubbles was reduced from 655 to 75 μm. Reis *et al*. [7] studied the effect of bubble size distribution on the flotation of fine apatite and found that maximum content of 60% P_2O_5 was achieved when fine apatite was floated by bubbles with a diameter less than 300 μm. This finding indicates that the collision and adhesion probabilities of fine particles to smaller bubbles are greater, which is beneficial for improving the flotation selectivity of fine minerals.

Microbubbles, micro–nanobubbles, and nanobubbles have many similarities, such as the preparation methods, availabil-

✉ Corresponding author: Ziyong Chang E-mail: changziyong@ustb.edu.cn
© University of Science and Technology Beijing 2023

ity in fine-particle flotation, and reduction of chemical consumption. In general, the smaller the air bubbles, the higher the preparation difficulty. Meanwhile, with the gradual reduction of the mineral particle size, the flotation machine/column is continuously improved. The combination of microbubbles, micro–nanobubbles, and nanobubbles with a flotation machine/column has become a hot topic in the flotation of ultrafine particles.

In the past few decades, several studies have been conducted by applying microbubble flotation for the beneficiation of fine particles. This work puts an emphasis on the latest development in the microbubble flotation machine/column and their application in the beneficiation of fine particles, including fine coals and metallic and nonmetallic minerals.

2. Preparation of microbubbles

2.1. Pressurized aeration and dissolved air

The principle of the pressurized aeration and dissolved air (PADA) method is to dissolve air in a slurry under high pressure and then release microbubbles in the flotation column after depressurization [8]. The value of air pressure has a great influence on the preparation of microbubbles. Typically, air is dissolved in the aqueous solution at 507 kPa, and an excess number of microbubbles will be produced if the air pressure is higher than this value. The PADA method can be used to produce microbubbles, micro–nanobubbles, and nanobubbles.

Han *et al*. [9] used the particle counter method to measure the size of bubbles produced by the PADA method. The results show that the bubble size gradually decreased when the air pressure increased from 101 to 355 kPa and plateaued with the further increase in air pressure. Gochin *et al.* [10] used the PADA method to evaluate the flotation of fine cassiterite and cassiterite–quartz mixtures and found that the method can be successfully used to separate fine minerals with high selectivity. The Sn grade increased from 7.4wt% to 60wt% after one rough and one cleaner separation, and the recovery of Sn was more than 60%, indicating that the PADA method is effective in the production of microbubbles and is promising for the beneficiation of fine minerals.

2.2. Electrolysis

The preparation of microbubbles via electrolysis involves placing electrodes in a pulp and electrolytically decomposing water into microbubbles containing hydrogen or oxygen. Electrolysis can be used to produce microbubbles, micro–nanobubbles, and nanobubbles with different sizes.

Tsave *et al.* [11] conducted a flotation of fine magnesite using microbubbles generated by electrolysis. The results show that the recovery of fine magnesite increased by 20% when electrolytic microbubbles were used in flotation, indicating that the presence of electrolytic microbubbles could significantly promote the flotation of fine particles. Generally, the recovery of fine particles is closely related to the current density and electrolysis time. However, electrolytic microbubble flotation is rarely used in mineral flotation because extremely fine bubbles cannot be easily produced.

2.3. Ultrasonic cavitation

A reduction in pressure makes a supersaturated liquid suffering from cavitation and generate nanobubbles [12]. At present, microbubbles produced via cavitation have been widely applied in fine- and coarse-particle flotation, high-intensity conditioning, oil agglomeration of fine coal, and high-efficiency oil sands processing [13].

Ultrasonic cavitation generates tensile stress and negative pressure in liquid, followed by the escape and release of air from the liquid. In the meantime, a strong tensile stress tears the liquid into cavities, and this process is known as cavitation. The small bubbles prepared via cavitation continue to grow, leading to the formation of several microbubbles. Microbubbles and micro–nanobubbles can be prepared via ultrasonic cavitation.

Chen *et al*. [14] found that microbubbles prepared by 600 kHz high-frequency ultrasound increased the recovery of fine particles by 30%, which was attributed to the increase in secondary acoustic radiation forces between the carriers, and high-frequency ultrasonic standing wave was likely to promote the attraction between carrier bubbles and circulating fluidized beds instead of repulsion. Peng *et al*. [15] investigated the effect of ultrasound on lignite flotation and found that ultrasonic treatment can generate a large number of microbubbles, which significantly enhanced the floatability of lignite by coating on the coal surface. This finding indicates that the ultrasonic synchronous flotation can greatly improve the clean coal yield and reduce the ash content simultaneously, compared with the conventional flotation. Kruszelnicki *et al.* [16] performed microflotation at different powers of applied ultrasound. Non-treated and ultrasound pre-treatment shale flotation tests were performed in the presence of methyl isobutyl carbinol (MIBC) frother and sodium ethylxanthogenate (KEX) collector, and they found that the mass recovery increased by 40% under 20 W applied ultrasonic power. Filippov *et al*. [17] found that compared with a reagent-only treatment, the flotation recovery of chalcopyrite after the ultrasonic treatment increased by 5%–20%, which is attributed to the promotion of the collision, adhesion, and coalescence of particles and bubbles by ultrasonic waves.

2.4. Photocatalysis

The principle of the photocatalysis method is to irradiate light with a certain wavelength on a photocatalytic material to generate an electron transition, thus producing and releasing microbubbles from the material surface once thermodynamic conditions reach the critical value [18]. Micro–nanobubbles and nanobubbles can be produced via photocatalysis.

Shen *et al*. [19] found that the surface of TiO_2 can generate hydrogen in a methanol/water solution through photocatalysis. Paxton *et al.* [20] successfully produced nanobubbles of H_2 and O_2 on the Pt electrode in 3.7wt% hydrogen peroxide aqueous solution.

2.5. Solvent exchange

By taking advantage of the solubility difference of air in variable solutions, microbubbles can be produced by substituting the solvent to release the saturated air, which is termed as the solvent exchange, including alcohol–water exchange, brine exchange, and cold and hot water exchange [21]. Alcohol–water exchange is the most frequently used owing to its high stability and good repeatability.

Lou *et al.* [22] successfully produced nanobubbles at a solid–liquid interface through an ethanol–water exchange. Guo *et al*. [23] used NaCl solution with a variable concentration to replace water and ethanol and generate nanobubbles.

2.6. Temperature difference method

Because the solubility of air in water decreases with increasing temperature, nanobubbles can be produced by dropping cold water onto the surface of hot substrate. Kyzas *et al*. [24] reported that the flotation performance of lignite was significantly improved after introducing nanobubbles generated by the temperature difference method (TDM), and the underlying mechanism was systematically investigated by studying the induction time and the collision–attachment behavior of bubbles and particles.

2.7. Venturi tube preparation method

The Venturi-type microbubble generator has attracted great attention due to its simple structure, high generation efficiency, and low energy consumption [25]. As shown in Fig. 1, when water flows through the throat of Venturi tube, air is sucked into the tube because the internal air pressure is much smaller than the atmospheric air pressure, followed by the breaking of air bubbles into microbubbles [26–27].

Ma *et al*. [28] placed Venturi tube at the bottom of flotation column to produce nanobubbles for fine-coal flotation and found that the presence of nanobubbles increased coal recovery by 10%–39%. Simultaneously, the dosage of the frother and collector was reduced by approximately 50%. Sakamatapan *et al.* [26] studied the effect of the flow speed on the number and size of microbubbles generated by the Venturi tube and found that the number of microbubbles gradually increased with an increase in the speed of water flow, whereas the bubble size gradually decreased. As reported by Xiong *et al*. [29], for the flotation of fine coal, an 11.7wt% concentrate assaying ash at combustible recovery of 86% was obtained when micro–nanobubbles generated by Venturi tubes accounted for approximately 70%. Wang *et al.* [30] used the Venturi tube to prepare nanobubbles to recover molybdenite. Their results showed that the introduction of nanobubbles can significantly increase the ultrafine molybdenite flotation recovery by almost 15.17%.

2.8. Swirl-type micro–nanobubble generator

As shown in Fig. 2, Wu *et al*. [31] developed a swirling micro–nanobubble generator by equipping a variable-pitch spiral cavitation reactor to enhance the shearing force of air bubbles. The variable-pitch spiral guide vanes and central column were installed into a cavitation reactor to generate a swirling liquid flow, thus intensifying the gas–liquid contact and mixing.

A computational fluid dynamics simulation indicated that

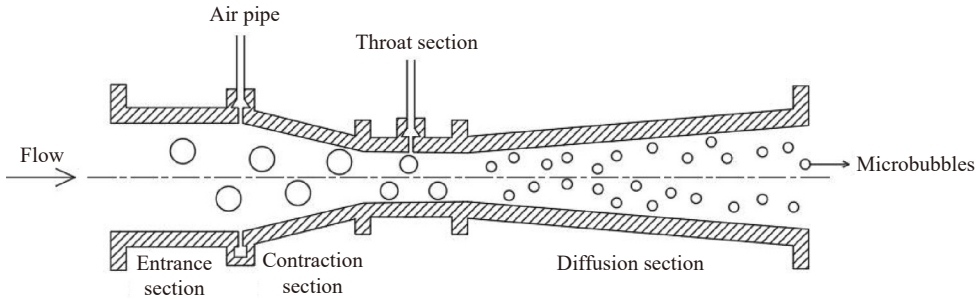

Fig. 1. Schematic diagram of the NBCF between two hydrophobic surfaces. Reprinted from *Adv. Colloid Interface Sci.*, 154, M.A. Hampton and A.V. Nguyen, Nanobubbles and the nanobubble bridging capillary force, 30, Copyright 2010, with permission from Elsevier.

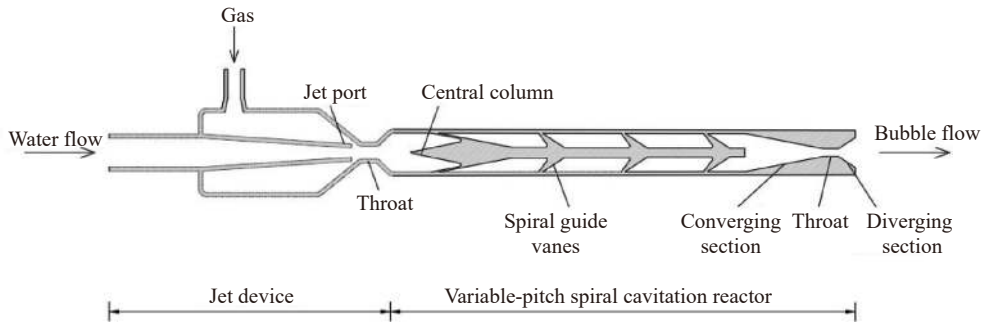

Fig. 2. Schematic diagram of the swirl-type micro–nanobubble generator. Reprinted from *Chem. Eng. Process.*, 181, M. Wu, H.Y. Song, X. Liang, N. Huang, and X.B. Li, Generation of micro–nano bubbles by self-developed swirl-type micro–nano bubble generator, 109136, Copyright 2022, with permission from Elsevier.

the manufactured bubble generator produced micro–nanobubbles with a minimum size and average size of 0.301 and 0.976 μm, respectively. In short, the swirl-type micro–nanobubble generator provides a guideline for the development of efficient micro–nanobubble generators.

2.9. Membrane method

The microbubbles produced by the membrane were formed by dispersing air through micropores on the porous membrane under a certain pressure [32]. In recent years, membrane dispersion technology based on porous membranes has attracted significant attention due to its controllable operating conditions, low energy consumption, and good dispersion [33].

Tao *et al*. [34] introduced a ceramic membrane sparger in the mineral flotation process. The strong fluid shear in the ceramic membrane channels and large porous area for gas dispersion make the recovery of fine quartz particles close to 100%. Because the size of microbubbles produced by microporous membranes is affected by the liquid flow velocity, liquid viscosity, surface tension, and membrane pore size, the microbubble size is difficult to control. Thus, to make the size of microbubbles stable and controllable, Xie *et al.* [35] developed a controllable preparation method for microbubbles using the ceramic membrane apparatus, which successfully prepared microbubbles with a diameter of 64–87 μm.

Above all, the PADA method is the most widely used in the preparation of microbubbles, micro–nanobubbles, and nanobubbles. Other methods are usually adopted to satisfy the specific requirements of the bubble size and application purposes. Generally, the PADA method and electrolysis can be used to produce all of three kinds of microbubbles, and photolysis and ultrasonic cavitation are used to produce micro–nanobubbles. Meanwhile, the solvent exchange and TDM are mainly used to prepare nanobubbles with the smallest bubble size. Table 1 summarizes the features of the microbubble preparation methods, including the respective average bubble size, mechanisms, advantages, and disadvantages. Generally, the PADA, electrolysis, ultrasonic cavitation, and swirl-type micro–nanobubble generator can produce microbubbles with a high bubble density and good dispersion. The advantages of photocatalysis, solvent exchange, and the TDM are convenience and high practicability. Moreover, microbubbles prepared by the Venturi tube and microporous membrane can easily control the bubble size. However, the primary limitations of these methods are their high energy consumption and limitations in the laboratory scale.

At present, the PADA has more application prospects in the microbubble flotation of fine minerals, which is worthy of great attention. The bottleneck problem restricted the application is that the air dissolution and release are not continuous and can easily cause corrosion, noise, and vibration. Thus, to break through the current situation of microbubble preparation, more efforts are needed to improve the design of pipes and cavitation devices. In addition, the flowrate and pressure of the solution should be more controllable.

3. Equipment for microbubble flotation

To promote the flotation of fine particles, a variety of microbubble flotation machines have been developed based on the principle of bubble preparation, including a microbubble release flotation machine, centrifugal flotation column, packed flotation column, and magnetic flotation machine.

3.1. Microbubble release flotation machine

A microbubble release flotation machine is the most promising equipment for fine-particle flotation. Bubbles released from an aqueous solution have small diameters, high dispersion rates, large surface areas, and preferentially adhere to hydrophobic mineral particles. Typically, microbubble release flotation machines mainly include a Jameson jet flotation column, a pressurized dissolved air flotation (DAF) machine, and an electroflotation column.

3.1.1. Jameson flotation column

The Jameson flotation column is widely used in fine-particle flotation owing to its flexible aeration mode and ex-

Table 1. Summary of the preparation methods for microbubbles

Preparation method	Average bubble size / μm	Mechanism	Advantage	Disadvantage
PADA	~70	Hydraulic cavitation method	Microbubbles with high bubble density	Discontinuous air dissolution and release
Electrolysis	~60	Electric	High dispersion concentration	High energy consumption
Ultrasonic cavitation	~65	Ultrasonic	Promote the dispersion of chemicals	High price of microwave generators
Photocatalysis	~0.015	Illumination	Easy to observe	Performance limited by materials
Solvent exchange	~0.1	Direct dropping method	Low cost	Easy to introduce impurity
TDM	~70	Temperature control method	Easy to operate	Low repeatability
Venturi tube preparation method	~90	Hydraulic cavitation method	Controlled bubble size	Limited in laboratory studies
Swirl-type micro–nanobubble generator	~0.976	Dispersed-air method	High oxygen enrichment capacity	Complex structure
Membrane method	~75	Pressure	High stability and controllability	High price and difficult production

cellent flotation performance. The schematic diagram of the Jameson flotation column is shown in Fig. 3 [36]. As can be seen, the slurry is fed into the ore port from the flotation column under a pressure of 0.1–0.15 MPa, and a jet is formed when passing through the nozzle. Air is sucked by a jet due to entrainment, leading to the formation of a partial vacuum in the lower pipe. As a result, air is continuously sucked into the slurry, followed by crushing into tiny bubbles under high pressure. Particles, bubbles, and water are fully mixed under vigorous mechanical stirring, contributing to the mineralization of bubbles. The uniformly mixed three-phase flow enters the flotation cell from the bottom of the lower conduit, and the mineralized bubbles rise up to form the foam layer. Finally, the valuable minerals overflow from the top of the flotation cell, and tailings are discharged from the bottom of the flotation cell [37].

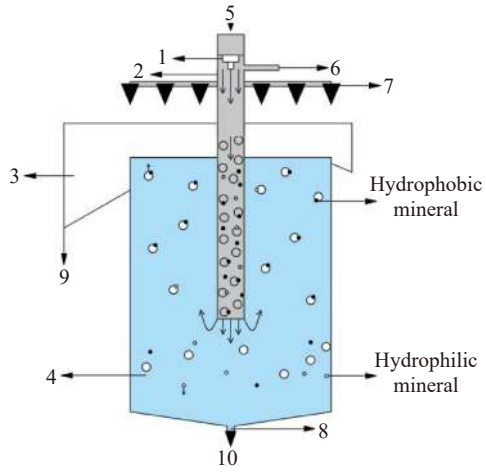

1-Feeding nozzle; 2-Lower pipe; 3-Concentrate chute; 4-Flotation cell; 5-Feeding; 6-Intake pipe; 7-Sprinkler; 8-Tailing pipe; 9-Concentrate; 10-Tailings.

Fig. 3. Schematic diagram of the Jameson flotation column. L.F. Zhou, L.H. Fu, and Q. Zhang, Efficient flotation column for fine particles, *Nonferrous Met.*, (2007), No. 2, p. 55.

Wang *et al*. [38] used the Jameson flotation column to float anthracite coal slime, and the ash content was significantly reduced from 29.5% to 10.28%, with a flotation yield of 61.43%. Zhou *et al*. [37] developed a new flotation column by designing a middling cycle system on the basis of the Jameson flotation column, and the feeding was introduced from the conical funnel at the lower part of the flotation cell. Li *et al*. [39] modified the Jameson flotation column to improve the flotation of spodumene in high-altitude areas. Microbubbles were produced by passing pressurized air through a microporous tube, thus eliminating the limitation of low air pressure and promoting bubble mineralization.

The Jameson flotation column can generate nanobubbles two orders of magnitude smaller than conventional bubbles, which is conducive to the flotation of fine particles [40]. A V-shaped bubble generator can produce several microbubbles [41], and the energy consumption is much smaller than that of conventional flotation columns [42].

The primary disadvantage of the Jameson flotation column is that the suction force will be significantly reduced once the pipes are exposed to air, or the nozzles cannot work well [43]. Moreover, it can easily cause a short circuit in the mineralized bubbles if the depth of the pipe inserted into the groove is too deep, leading to the loss of valuable minerals in the tailings. In addition, the flotation recovery is always reduced due to the lack of a middling circulation device.

3.1.2. Pressurized DAF column

As mentioned above, numerous microbubbles can be produced by the PADA method, which is conducive to the flotation of fine particles. As shown in Fig. 4, the Mechanical Research Institute of Beijing General Research Institute of Mining and Metallurgy (BGRIMM) has developed a pressurized DAF machine for fine-particle separation [44]. An air-saturated slurry is formed under 2.02×10^5–3.03×10^5 Pa, and air will be completely released once reduced to 101 kPa. Meanwhile, microbubbles preferentially adhere to hydrophobic mineral particles.

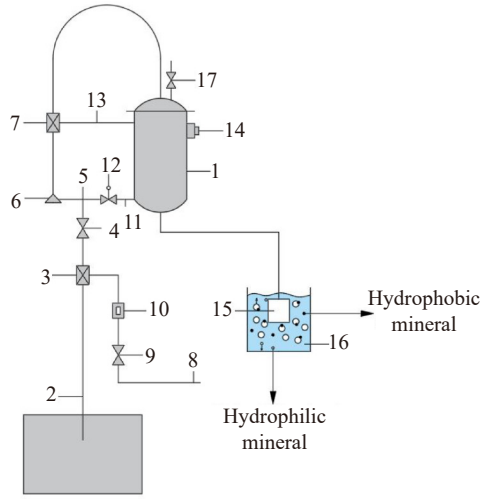

1-Air saturator; 2-Inlet pipe; 3-Ejector; 4-Back-pressure valve; 5-Three way pipe; 6-Pump; 7-Ejector; 8-Air duct; 9-Flow control valve; 10-Float flowmeter; 11-Pressurized circulating tube; 12-Electromagnetic valve; 13-Circulating air tube; 14-Liquid level controller; 15-Releaser; 16-Release corner; 17-Safety valve.

Fig. 4. Schematic diagram of the PADA. Reprinted from *J. Water Process Eng.*, 32, C. Wang, Z. Wang, X. Wei, and X. Li, A numerical study and flotation experiments of bicyclone column flotation for treating of produced water from ASP flooding, 100972, Copyright 2019, with permission from Elsevier.

Within the pressurized DAF column, the slurry is embedded into a dissolved air container under a certain pressure, and a negative pressure will be formed during this process. Air is continuously inhaled from outside under the high-speed slurry flow to form a saturated air solution via sufficient mixing, and it will be released from the slurry to generate microbubbles once switched on the control valve. Microbubbles prefer to adhere to hydrophobic mineral particles, and non-adhered microbubbles and mineral particles suspended in a turbulent water flow collide and adhere to one another when passing through the dissolved gas releaser, thereby realizing bubble mineralization.

Sun *et al*. [45] found that the size of microbubbles produced by the PADA is much smaller than that produced using an agitation flotation machine, and the distribution of microbubbles in a slurry is in good agreement with the normal distribution. Yoshikawa *et al*. [46] reported that a pressurized DAF machine showed a higher separation ability than the Denver flotation machine with less sodium oleate consumption for the beneficiation of barite–quartz.

3.1.3. Electroflotation column

For the electroflotation column, microbubbles are produced via electrolysis and are closely related to the current magnitude [3]. As shown in Fig. 5, the electrolytic microbubble generator and feeding port are set at the top of the flotation column, and a stirrer is installed at the bottom of the flotation column to promote the collision between mineral particles and air bubbles [47]. The hydrophobic particles adhere to the microbubbles to form particle–bubble aggregates and enter the foam layer, finally being collected as a concentrate. The hydrophilic particles cannot attach to microbubbles and are discharged as tailings from the top of the column.

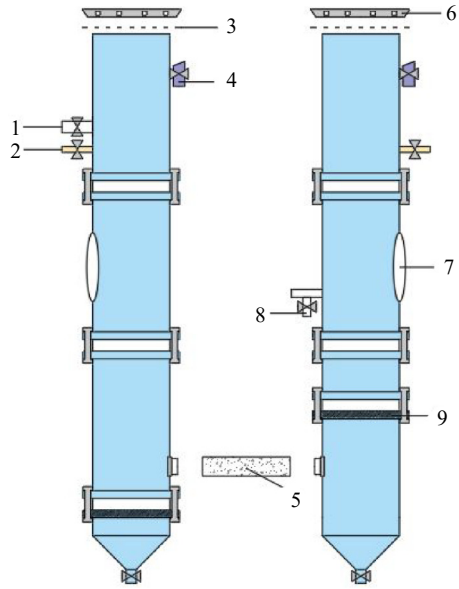

1-Feed inlet; 2-Adding-reagent inlet; 3-Sieve net; 4-Outlet; 5-Sand-core salt bridge; 6-Sealed cap; 7-Horizontal observation hole; 8-Sample connection; 9-Electrode.

Fig. 5. Schematic representation of the "U"-type electroflotation setup. W. Zhao, J.Z. Qu, Z. Li, Z.Y. Yang, and A.N. Zhou, Influencing factors of electroflotation–electrocoagulation seperation of coal macerals, *Clean Coal Technol.*, 24(2018), No. 1, p. 57.

Yang *et al*. [48] used an electroflotation column to recover scheelite from tungsten tailings and found that compared with the conventional flotation machine, the concentrate grade and recovery of tungsten obtained by the electroflotation column increased by 0.57wt% and 8.54%, respectively. Yang *et al.* [48] designed a new electroflotation column to recover fine ilmenite with a titanium grade of 10.67wt%, and a rough concentrate assaying TiO_2 at 19.90% at a recovery of 60.65% was obtained. At present, an electroflotation column has been widely used in the electrolytic flotation of scheelite.

An electroflotation column can produce uniform microbubbles with controllable quantity, and the intercalation of gangue particles can be effectively reduced through vigorous mechanical stirring. A slurry flow has high stability, which is conducive to froth flotation and secondary enrichment. The primary shortcomings of the electroflotation column are the fluctuating operation conditions, high energy consumption, and easy blockage.

3.2. Centrifugal flotation column

The centrifugal flotation column improves the flotation of fine particles by taking advantage of the centrifugal force. Typically, cyclone-static microbubble flotation column (FCSMC) developed by China University of Mining and Technology has been widely applied in the flotation of fine particles.

Owing to the unique three-stage separation zone, the FCSMC has exhibited great advantages in the beneficiation of fine particles [49]. As shown in Fig. 6, the FCSMC is composed of a column unit, cyclone unit, and pipe unit [50]. In the column unit, particles with high hydrophobicity attach to the rising air bubbles and float up to enter the concentrating collector, whereas the rest of the mineral particles fall off into the cyclone unit. The inverted cone on the top of the cyclone unit makes the unit work like a hydrocyclone. Mineral particles with medium hydrophobicity are collected as middling under high-intensity swirling, whereas the hydrophilic particles are discharged as tailings. Subsequently, the mid-

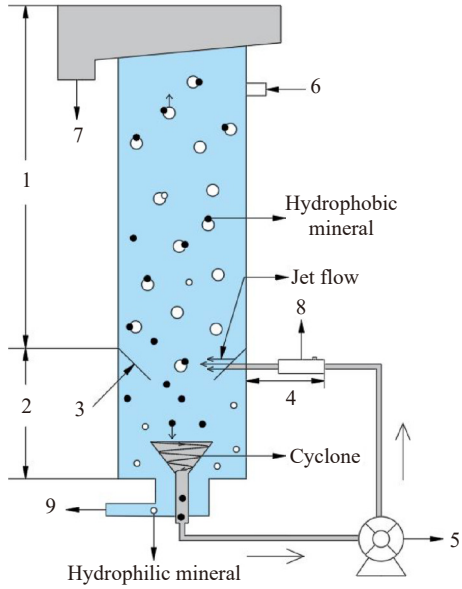

1-Column unit; 2-Cyclone unit; 3-Cyclone inverted cone; 4-Pipe unit; 5-Circulating pump; 6-Feed; 7-Concentrate; 8-Bubble generator; 9-Tailing.

Fig. 6. Schematic of the cyclone-static microbubble flotation column. Copyright ©2018. John Wiley and Sons. Reproduced from X.K. Yan, S.Q. Meng, A. Wang, L.J. Wang, and Y.J. Cao, Hydrodynamics and separation regimes in a cyclonic-static microbubble flotation column, *Asia Pac. J. Chem. Eng.*, 13(2018), No. 3, art. No. e2185.

dling is pumped into the pipe unit and flows through the bubble generator, thus colliding with microbubbles [51].

Miller *et al.* [52] found that the FCSMC can extend the lower particle size limit for effective flotation by combining nanobubbles and centrifugal force separation. Zhou *et al.* [53] conducted a semi-industrial test on the rough separation of scheelite using the FCSMC. They found that the grade of a rough concentrate reached 9.76wt%, while the grade of the tailings was reduced to 0.10wt% after a 72 h continuous closed-circuit flotation. The FCSMC had little effect on the recovery of scheelite, but it greatly simplified the flotation process and reduced the flotation cost. Deng *et al.* [54] studied the flow field of the cross-section and longitudinal section of the cyclone flotation zone using the FCSMC and found that the combined swirl of the transverse and longitudinal sections is conducive to the beneficiation of fine particles.

Compared to the conventional flotation column, the FCSMC is more energy-saving with lower operating costs because it does not use mechanical stirring to disperse air, and the non-selective hydraulic entrainment of fine particles is reduced due to superior hydrodynamic conditions. However, the FCSMC still consumes lots of water for the separation of fine particles, which is not applicable in drought and scarce areas. Moreover, some parts of the equipment are easy to wear [55].

3.3. Packed flotation column

In recent years, porous materials have frequently been packed in columns to generate microbubbles for the flotation of fine particles, which is named the packed flotation column [56]. Slurries and bubbles flow in the opposite direction in a packed flotation column, which is similar to the conventional flotation column. As shown in Fig. 7, the primary difference is that the packed flotation column is packed with a porous medium in the inner shaft, which are arranged layer by layer at an angle of 90° to provide small tortuous flow channels for the close contact between particles and air bubbles, thereby improving the separation of foam [57–58]. The packed flotation column has a good aeration performance, which can work continuously and is easy to adjust, leading to the formation of a stable foam layer on the pulp surface. The separator in the packing layer breaks large bubbles into tiny bubbles and prevents them from merging, which increases the trapping area in the flotation column. As a result, the packed flotation column can generate smaller bubbles than the conventional flotation column, thereby greatly increasing the contact chance of bubbles with fine particles and improving the recovery and flotation selectivity of fine particles. Nowadays, packed flotation columns have been widely used in the chemical industry [59].

Wang *et al.* [60] used a packed flotation column to perform the reverse flotation of fine hematite with a feed grade of 42.15wt%, and a concentrate assaying Fe (67.05wt%) was obtained after one roughing, one refining, and one sweeping. The tailing grade was reduced to Fe 11.25wt%, indicating that the packed flotation column was effective for the flotation of fine-grained hematite. Zhang *et al.* [61] studied the flotation of fine-grained bauxite ore using a plate-packed flotation column and found that the recovery and grade of Al_2O_3 increased by 2.11% and 1.85wt%, respectively. Correspondingly, the fraction of 20 μm particles in the concentrate increased from 47.31% to 54.79%. Zhang *et al.* [62] packed fluid guiding media in a flotation column, which simultaneously increased the gas holdup in the column separation area and reduced the bubble size. As a result, the copper recovery of low-grade copper sulfide ore increased from 91.73% to 92.92%.

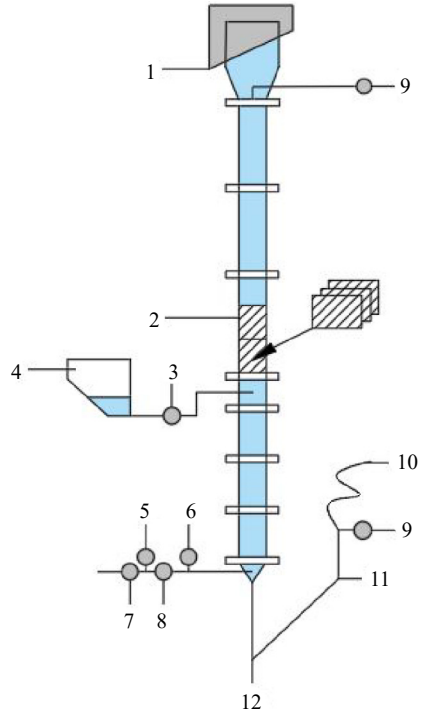

1-Concentrate; 2-Paked medium; 3-Pump; 4-Mixer; 5-Compressed air; 6-Pressure gange; 7-Pressure reducer; 8-Flowmeter; 9-Water; 10-Liquid level control; 11-Floemeter; 12-Tailing.

Fig. 7. Packed flotation column. B. Wang and H. Jiang, Research and application of flotation column, *Chin. J. Nonferrous Met.*, 31(2021), No. 4, p. 1027.

The primary disadvantage of a packed flotation column is that a high column body is not conducive to the operation, and the long residence of fine particles in the column will cause mineral oxidation, which is not suitable for the separation of sulfide minerals.

3.4. Magnetic flotation machine

3.4.1. Yalcin magnetic flotation machine

A magnetic flotation machine is composed of uniform and nonuniform magnetic fields. In the uniform magnetic field, magnetic particles undergo selective magnetic agglomeration, which is conducive to froth flotation by increasing the apparent particle size. While in a nonuniform magnetic field, magnetic particles are separated from nonmagnetic particles via magnetic separation. Therefore, the separation of fine magnetic and nonmagnetic particles can be enhanced by the combination of froth flotation and magnetic separation.

Fig. 8 shows a magnetic flotation machine developed by Yalcin for the reverse flotation of fine magnetic minerals [63]. The magnetic flotation machine is composed of foaming and flotation areas. During the flotation process, hydrophobic mineral particles move toward the foaming area after adhering to the bubble surface. The mineralized particles break when encountering flushing water, and mineral particles fall off from the air bubbles to the chamber below. The magnetic particles in the froth are carried back to the flotation zone by rotating magnets, which are in the opposite direction of the froth flow. The separation process is completed when air bubbles do not carry nonmagnetic particles anymore, and the stable foam layer disappears, which can improve the separation of magnetic particles from nonmagnetic particles [64]. Furthermore, the Yalcin magnetic flotation machine simplifies the process by reducing the processing times of intermediate materials and has the advantages of low energy consumption and steady operation. The primary disadvantage is that the reduction of nonmagnetic particle entrainment requires a lot of flushing water, which increases water consumption and is not applicable in dry areas.

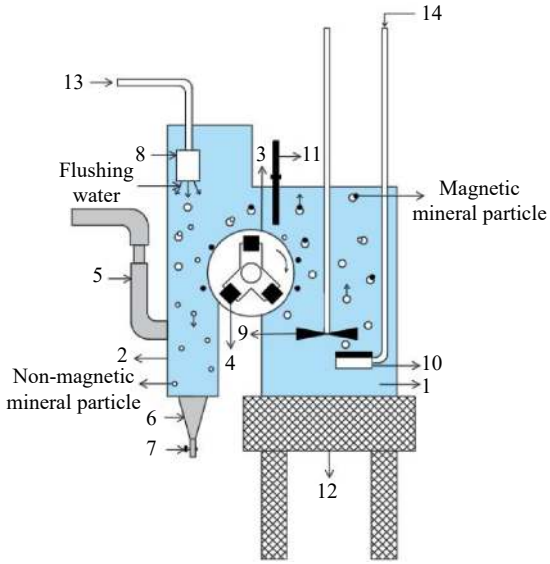

1-Flotation compartment; 2-Forth product compartment; 3-Circular tubing; 4-Magnet assembly; 5-Overflow pipe; 6-Drainage pipe; 7-Clamp; 8-Water spray box; 9-Impeller; 10-Air bubble; 11-Froth paddle; 12-Support platform; 13-Water inlet; 14-Compressed air inlet.

Fig. 8. Yalcin magnetic flotation machine. S. He and B.C. Chen, Discussion on flotation machine for ores, *China Min. Mag.*, 3(1994), No. 4, p. 31.

3.4.2. Magnetic flotation column

The novel magnetic flotation column developed by BGRIMM is shown in Fig. 9, which is mainly used for the separation of strong magnetic minerals and nonmagnetic gangue minerals [65]. A pulsed alternating electromagnetic field with a tunable pulse time and magnetic intensity in a certain range is adopted in the column. As shown in Fig. 10, the magnetic particles are in a state of "dispersion–agglomeration–dispersion" and change alternately with the magnetic intensity, destroying the magnetic flux under a pulsed magnetic field. Nonmagnetic and poor magnetic particles are separated from magnetic particles under the combination of buoyancy, gravity, and the flush force of rising water. Nonmagnetic minerals are separated from the magnetic chain and float up after being captured by air bubbles. Then, the mag-

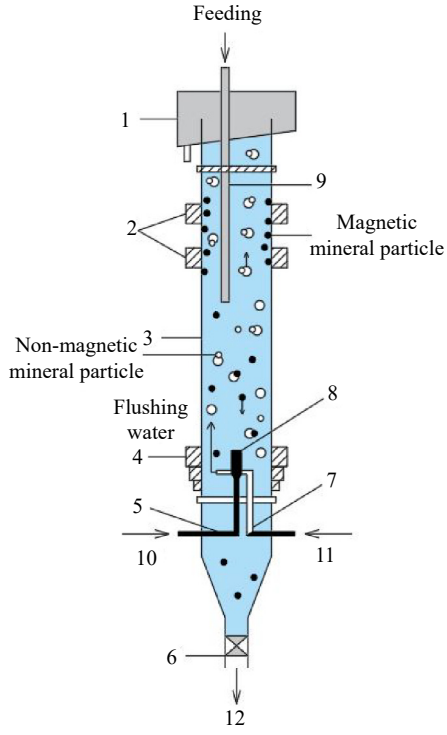

1-Overflow tank; 2-Pulse electromagnetic coil; 3-Sorting column; 4-Demagnetization coil; 5-Inflation tube; 6-Ore discharge outlet; 7-Water inlet pipe; 8-Air separator; 9-Feed pipe; 10-Air; 11-Water supply; 12-Ore discharge.

Fig. 9. Magnetic flotation column. S.X. Shi, L.J. Yang, Z.C. Shen, and S.J. Lu, Research status of fine particle flotation beneficiation methods and equipment, [in] *Proceedings of the Proceedings of the Fifth National Conference on Mining and Dressing Technology Progress*, Hohhot, 2006, p. 121.

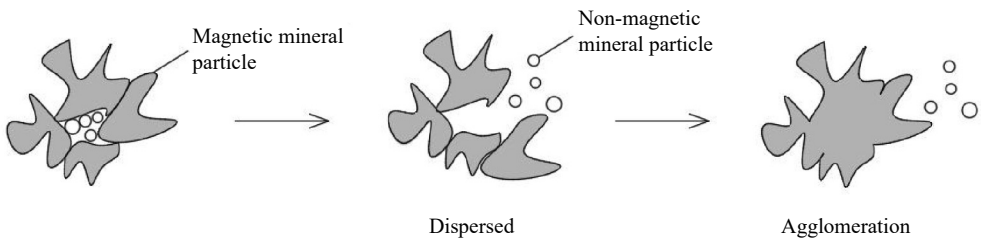

Fig. 10. Dispersion–agglomeration state of magnetic particles.

netic particles are discharged under the influence of magnetic and gravity forces. Magnetic minerals cannot be easily carried into the foaming area by bubbles because they are trapped when passing through the magnetic field, which plays a depressant role for magnetic minerals [66].

Deng *et al*. [67] developed a three-product magnetic flotation column for the separation of chalcopyrite–pyrrhotite ores and found that the Cu grade increased from 14.20wt% to 26.40wt% when a magnetic field was adopted, whereas the S recovery decreased from 89.6% to 34.3%, suggesting that the magnetic field improved the separation efficiency of pyrrhotite from chalcopyrite. Liao *et al*. [68] used a flotation column with six external coils for the flotation of iron ores and found that the pulse magnetic field increased the recovery and grade of Fe in the concentrate by 1.12% and 4.22wt%, respectively, compared to the conventional flotation column. Table 2 summarizes the microbubble flotation equipment from different aspects, including the air charging mode, movement direction of bubbles and pulp, and application directions.

Table 2. Summary of microbubble flotation equipment

Microbubble flotation equipment	Air charging mode	Movement direction	Applications
Jameson flotation column	External inflatable	Concurrent flow	Coal slime
Pressurized DAF column	External inflatable	Countercurrent flow	Iron ore/quartz
Electroflotation column	Internal inflatable	Countercurrent flow	Scheelite/ilmenite
Packed flotation column	Internal inflatable	Countercurrent flow	Hematite/fluorite/bauxite
Yalcin magnetic flotation machine	External inflatable	Countercurrent flow	Magnetic ore
Magnetic flotation column	External inflatable	Countercurrent flow	Magnetic ore
Centrifugal flotation column	External inflatable	Counter-cocurrent mixed	Metallic ores/nonmetallic ores/coal

4. Application of microbubble flotation in practice

At present, microbubble flotation has exhibited unique technical advantages and promising application prospects in the flotation of fine coals and fine minerals.

4.1. Fine-coal flotation by microbubbles

With the development of coal mining mechanization, the proportion of fine coals with particle size <0.074 mm and muddy substance with high ash content has rapidly increased, leading to the gradual deterioration of coal floatability [69]. The flotation efficiency and performance of fine coals by conventional flotation machines significantly decreased due to the gradual increase of the coal slurry concentration [70]. Moreover, the microbubble flotation column has been widely used in fine-coal flotation owing to its unique working mode and excellent flotation performance [71].

Fan *et al*. [72] reported that the presence of nanobubbles could significantly reduce the average particle size of ultrafine coal flotation concentrates from 103 to 69 μm, indicating that nanobubbles can effectively improve the flotation of fine-coal particles. Li *et al.* [73] prepared nanobubbles via the TDM for the flotation of ultrafine coal. They found that the flotation yield of ultrafine coal was increased by up to 15%, and the flotation rate constant was also significantly enhanced. Sobhy *et al.* [74] used a flotation column equipped with Venturi tube to float fine coal in Illinois and found that the flotation recovery of fine coal was increased from 45% to 50%.

4.2. Flotation of ultrafine metallic minerals

4.2.1. Flotation of fine oxidized minerals

Zhang *et al.* [75] used benzhydroxamic acid as the collector for the flotation of fine rutile and found that the flotation recovery and flotation rate were significantly increased with less collection after pretreating rutile with nanobubbles. Tao *et al.* [76] studied the effect of nanobubbles on the flotation of hematite using a mechanical flotation cell integrated with a cavitation device. The results show that nanobubbles can significantly improve the concentrate grade and recovery of hematite. As reported by Fan *et al*. [77], compared with the conventional flotation machine, the FCSMC increased the concentrate grade and recovery of fine ilmenite by 1.08wt% and 13.64%, respectively. Moreover, the flotation process was simplified from the original "one roughing, two scavenging, and three cleaning" to "one roughing and one cleaning" process.

4.2.2. Flotation of fine sulfide ores

Ahmadi *et al*. [78] found that the existence of micro–nanobubbles increased the recovery of chalcopyrite fine particles ((−38 + 14.36) μm) and ultrafine particles ((−14.36 + 5) μm) by 16%–21%, and the recovery of ultrafine particles was higher than that of fine particles. Then, they conducted the modeling and optimization of the nanobubble generation process for the flotation of fine chalcopyrite and found that the minimum median nanobubble size was 130.75 nm for effective nanobubble flotation [79]. Cheng *et al*. [80] found that the swirl injection flotation column was much more effective for the flotation of −19 μm pyrite than the conventional flotation machine. Chipakwe *et al*. [81] reported that the introduction of nanobubbles could significantly improve the flotation performance of complex Pb–Cu–Zn sulfide ores.

4.2.3. Flotation of other fine metallic minerals

Cao *et al*. [82] found that the grade of rough copper concentrate obtained by a column flotation cell micro-fine flotation machine was 3%–6% higher than that obtained by a mechanical stirring flotation machine, and the beneficiation

efficiency was 5.19%–5.59%. Wei *et al.* [83] reported that the recovery of fine wolframite with a particle size smaller than 20 μm increased by 12.04% after introducing nanobubbles into the flotation system. Overall, microbubbles can significantly increase the collision probability between air bubbles and mineral particles, thereby improving the selectivity and floatability of fine metallic minerals.

4.3. Flotation of fine nonmetallic minerals

Slime coating has significantly deteriorated the flotation of nonmetallic minerals due to the ultrafine dissociation of mineral particles, thus reducing the flotation selectivity [84]. In recent years, the microbubble flotation column has exhibited great promise in improving the flotation of fine nonmetallic minerals.

4.3.1. Flotation of fine fluorite

Wang *et al.* [85] separated fluorite from scheelite tailings using a microbubble flotation column, and a concentrate assaying 99.01wt% CaF_2 with a recovery of 40.11% was obtained, which significantly improved the concentrate grade and recovery compared to the conventional flotation machine. As reported by Chen *et al.* [86], compared with the traditional mechanical flotation, the grade and recovery of fluorite obtained by the FCSMC were increased by 0.67wt% and 0.35%, respectively.

4.3.2. Flotation of fine quartz

Farrokhpay *et al.* [87] studied the effect of microbubbles on the flotation of fine quartz. They found that microbubbles (<50 μm) were effective in the flotation of fine quartz, which was difficult to float by conventional bubbles, and the equivalent or even higher recovery of quartz can be achieved using fewer collectors. In addition, the flotation rate of quartz increased with the use of microbubbles. The high quartz flotation rate in the presence of microbubbles was mainly attributed to the high adhesion efficiency of particles to microbubbles. Calgaroto *et al.* [88] found that nanobubbles could increase the contact angle at the quartz/water interface and improve the flotation recovery of ultrafine quartz, which was attributed to the enhancement of mineral hydrophobicity and aggregation of ultrafine quartz particles. Rosa *et al.* [89] studied the effect of nanobubbles on the flotation of quartz and apatite and found that the flotation recovery of quartz and P_2O_5 were increased by 23% and 9% after conditioning with nanobubbles, respectively, which were ascribed to the enhanced adhesion of air bubbles onto quartz and apatite by attached nanobubbles.

4.3.3. Flotation of fine graphite

Bu *et al.* [90] reported that the flotation column exhibited a high cleaning efficiency for graphite because it was equipped with a centrifugal force field, nanobubbles, and a thick foam layer, and the ash content of graphite was reduced by approximately 5%. Ma *et al.* [91] used a high-pressure grinding roller and a stirred mill to grind graphite to 0.045–0.15 mm, followed by flotation using the nanobubble flotation column. Consequently, a concentrate assaying 94.82% carbon at a recovery of 97.89% was obtained.

The application of microbubbles in the flotation of fine coal, metallic minerals, and nonmetallic minerals is summarized in Table 3. Overall, microbubbles can effectively improve the flotation performance of fine particles with high flotation recovery, high selectivity, and less chemical consumption.

5. Interactions between nanobubbles and fine particles

The flotation of mineral particles by air bubbles can be further divided into three subprocesses: collision between particles and air bubbles, adhesion of particles to air bubbles, and float-up of bubble–particle aggregates into foam layers [28]. A stable mineralized foam was obtained. In particular, the adhesion of particles to bubbles is considered the most important and most complicated, which is the key to determining the overall flotation efficiency of mineral particles.

Table 3. Summary of the application of microbubbles in the flotation of fine particles

Fine particle	Size / mm	Weight percentage / wt%	Equipment	Average bubble size / μm	Flotation recovery / %	Ref.
Coal	−0.045	48	Jameson flotation column	~400	80.00	[92]
	−0.025	41	Venturi tube	~1	50.00	[74]
	−0.045	65	Hallimond tube	~0.5	77.00	[73]
Gold	−0.045	70	FCSMC	~300	88.15	[93]
Copper sulfide	—	—	FCSMC	~300	93.66	[94]
Pyrite	−0.019	87	FCSMC	~300	60.00	[80]
Hematite	−0.0308	49.67	FCSMC	~300	86.06	[95]
	−0.053	46.79	FCSMC	~300	79.22	[96]
Molybdenum	−0.038	84.00	FCSMC	~300	62.71	[97]
Chalcopyrite	−0.01978	68.10	Microbubble generator	0.358	99.09	[78]
Graphite	−0.045	80.39	FCSMC	~300	98.77	[98]
Bauxite	−0.023	53.43	FCSMC	~300	85.65	[99]
Apatite	—	—	DAF	~100	76.68	[100]
Phosphate	—	—	Specially designed flotation column	~0.8	98.00	[101]
Quartz	0.020–0.050	—	Microbubble generator	~50	90.00	[87]

Owing to the nanometer-sized diameter, nanobubbles display a unique behavior during their interactions with fine particles.

5.1. Effect of nanobubbles on the agglomeration of fine particles

Nanobubbles can promote the agglomeration of fine particles and enhance their attachment to air bubbles, thereby improving the flotation performance [102]. As reported by Buchmann *et al*. [103], the agglomeration of solid particles in an aqueous solution is significantly influenced by their mutual interactions, such as electrostatic interactions, van der Waals force, and hydrophobic interaction. For hydrophobic particles, the interaction forces can be dramatically increased by nanobubbles at the particle surface due to capillary bridges [104]. As shown in Fig. 11, as the hydrophobic particles approach, the nanobubbles on their respective surfaces interact with one another and join to form a capillary bridge [105]. The resultant nanobubble bridging capillary force (NBCF) increases the contacts of different particles, thereby promoting particle agglomeration. In addition, Rulyov [106] proposed the theory of combined microflotation, which accurately describes the hetero-aggregation of particles and fine bubbles in the nonuniform hydrodynamic field of a flotation cell. Based on reports, the capture efficiency of fine particles by fine bubbles is about 15 times higher than that by coarse bubbles. The flotation rate of mineral particles deposited on slowly rising fine bubbles and then on the coarse bubbles is higher than that directly deposited on rapidly rising coarse bubbles.

Several experimental measurements and theoretical calculations have confirmed that nanobubbles can increase the attraction between two hydrophobic solids in an aqueous solution. Ditscherlein *et al.* [107] reported that pre-existing nanobubbles promote the adhesion between alumina particles. Knüpfer *et al*. [104] studied the agglomeration behavior of particles in the presence of nanobubbles through dynamic image analysis and found that the formed agglomerates were compact with fractal or porous shapes, varying from round to elongate. Li *et al*. [108] found that deaeration improved the settling efficiency of coal particles in water and reduced the size of coal agglomerates, which was attributed to the generation of nanobubbles on coal surfaces via immersion, allowing coal particles to easily agglomerate and contributing to the improvement of the coal flotation performance. Similar aggregation behavior of quartz particles in the presence of nanobubbles was also reported by Calgaroto *et al*. [88]. Overall, the presence of nanobubbles can increase the apparent particle size by promoting agglomeration, thus promoting the collision probability of particles and air bubbles, which is an important reason for the improved flotation performance of fine particles.

5.2. Effect of nanobubbles on the contact angle of mineral surfaces

The floatability of minerals is closely related to the wettability of mineral surfaces, and the contact angle is one of the most important criteria used to assess the wettability of mineral surfaces. Based on the literatures, the introduction of nanobubbles can significantly improve the contact angle of mineral surfaces, thus enhancing the floatability of fine particles [109].

Moreover, the three-phase contact angle of nanobubbles is much larger than that of macrobubbles [110]. Generally, individual macrobubbles directly attach to the solid surface with a limited contact angle and contact area. After pretreating solids with nanobubbles, individual macrobubbles prefer to coalesce with nanobubbles first and then attach to the solid surface, thereby increasing the contact angle and contact area between air bubbles and mineral particles [111]. Fig. 12 shows the contact angles of highly oriented pyrolytic graphite (HOPG), dodecyl trichlorosilane-modified silicon, and octadecyl trichlorosilane (OTS)-modified silicon [112]. Among the three solid surfaces, the nanocontact angle of the HOPG is the largest, and the macrocontact angle is the smallest. Furthermore, the difference between the nano- and macrocontact angle decreases as the macrocontact angle increases. Ren *et al*. [113] pretreated a polished massive cassiterite in different solution conditions. A high-speed camera was used to record images and calculate their contact angle, and the results are shown in Fig. 13. The contact angles of cassiterite in ultrapure water, 50 $mg \cdot L^{-1}$ octanohydroxamic acid aqueous solution, and 50 $mg \cdot L^{-1}$ octanohydroxamic acid micro–nanobubble aqueous solution were 40°, 62°, and 79°, respectively. This finding indicates that the introduction of micro–nanobubbles could significantly increase the contact angle of cassiterite in the presence of octyl hydroxamic acid. An *et al.* [114] reported that the contact angle of nanobubbles on a mineral surface is usually in the range of 150°–160°, as observed using an atomic force microscope (AFM). Johnson *et al*. [115] reported that the contact angle of nanobubbles on the membrane is about 165°, which is twice more than the contact angle of macrobubbles of 72.6°. Moreover, the appearance and morphology of nanobubbles

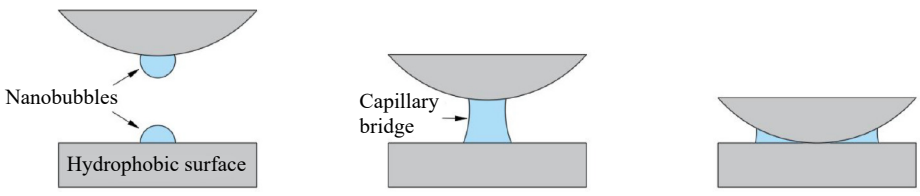

Fig. 11. Simplified mechanism of the NBCF between two hydrophobic surfaces. Reprinted from *Adv. Colloid Interface Sci.*, 154, M.A. Hampton and A.V. Nguyen, Nanobubbles and the nanobubble bridging capillary force, 30, Copyright 2010, with permission from Elsevier.

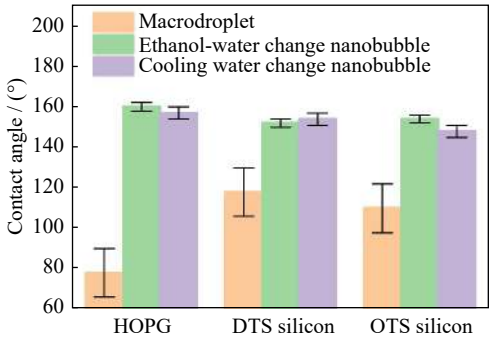

Fig. 12. Comparison between the contact angle of nanobubbles generated by different methods on three different substrates and the contact angle of macro droplets. Reprinted from *Miner. Eng.*, 183, D. Tao, Recent advances in fundamentals and applications of nanobubble enhanced froth flotation: A review, 107554, Copyright 2022, with permission from Elsevier.

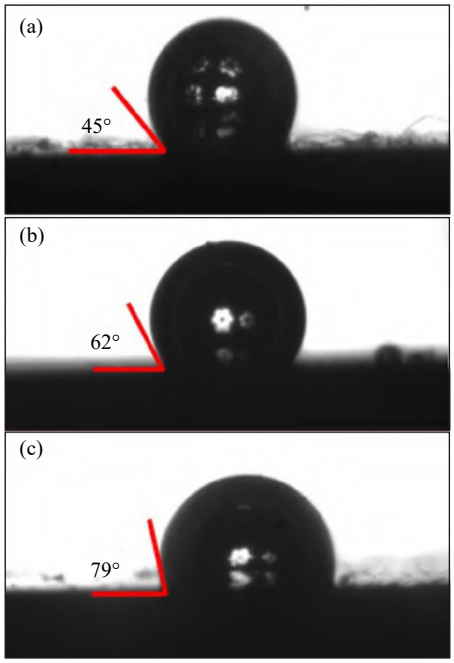

Fig. 13. Contact angle of the mineral surface under different conditions: (a) ultrapure water; (b) 50 mg·L^{-1} octanohydroxamic acid aqueous solution; (c) 50 mg·L^{-1} octanohydroxamic acid micro–nanobubbles aqueous solution. L.Y. Ren, W.N. Zeng, Z.Y. Zhang, and P.G. Wei, Visualization of the effect of micro–nano bubbles on aggregation of fine cassiterite, *Chin. J. Nonferrous Met.*, 32(2022), No. 5, p. 1479.

on hydrophobic surfaces are different from those of microbubbles. Based on the AFM images, surface nanobubbles are usually spherical and cap shaped. The height of nanobubbles is usually in the range of 10–100 nm, and the radius is in the range of 50–500 nm [116]. With the increase in interfacial hydrophobicity, the contact angle difference between nanobubbles and large bubbles significantly increased [76]. In the flotation process, the existence of nanobubbles on the surface of hydrophobic particles can magnify the hydrophobicity difference between valuable and gangue minerals, thus increasing the flotation selectivity of fine particles [117].

5.3. Effect of nanobubble stability on mineral flotation

The stability of nanobubbles has always been controversial and has attracted widespread attention [118]. Theoretically, nanobubbles are thermodynamically unstable due to their huge internal pressure [119]. According to Fick's second law and Henry's law, nanobubbles with a radius of 10 nm can only exist in solutions by 1 μs [120]. However, many experimental studies indicate that nanobubbles have long-term retention on hydrophobic particle surfaces.

Ishida *et al*. [121] immersed a silicon wafer hydrophobized with OTS into the water and found that numerous nanobubbles were generated on the silicon surface and lasted for hours. Azevedo *et al*. [122] studied the generation of nanobubbles and their physicochemical and interfacial properties and found that the mean diameter and concentration of nanobubbles only slightly varied in 14 d, demonstrating that the highly concentrated nanobubbles possessed extremely high stability in aqueous solutions. Many models and theories, such as the impurity layer [123], dynamic equilibrium [124], dense gas layer [125], linear tension [126], and contact line pinning [127], have been proposed to account for the high stability of nanobubbles. Based on the dynamic equilibrium model shown in Fig. 14, Seddon *et al*. [128] proposed that nanobubbles can exist in the form of dynamic equilibrium. Gas molecules cannot interact with one another at the liquid–gas interface due to their Knudsen behavior and flow directly away from the substrate (Fig. 14(a)). The bulk velocity of gas molecules can be decomposed into normal and tangential components. The tangential velocity of gas molecules always points toward the apex of the bubble and combines with the liquid phase via the assumed continuity of shear-stress boundary conditions (Fig. 14(b)). A local circulatory stream was created by the liquid flow tangential to the

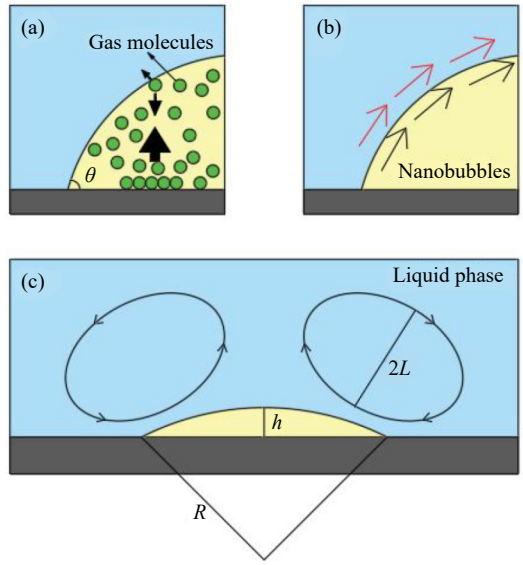

Fig. 14. Dynamic equilibrium model diagram for the stability of nanobubbles. Reprinted with permission from J.R.T. Seddon, H.J.W. Zandvliet, and D. Lohse, Knudsen gas provides nanobubble stability, 107, 116101. Copyright 2011 by the American Physical Society.

liquid–gas interface due to the mass conservation. Finally, the dissolved gas in the liquid phase re-enters nanobubbles through either the attractive potential of the hydrophobic wall or through adsorption to the substrate and surface diffusion. Among them, 2*L* refers to the inner diameter of the radial circulation of liquid flow (Fig. 14(c)).

The stability of nanobubbles has a significant effect on the flotation behavior of mineral particles. As mentioned above, the presence of nanobubbles can help enhance the hydrophobicity of mineral particles and improve the flotation selectivity. In addition, the effective hydrophobic agglomeration of particles is closely related to the stable existence of nanobubbles at the solid–liquid interface. Therefore, the long-term retention of nanobubbles at the hydrophobic particle surface enhances the stability and strength of hydrophobic aggregates, thus improving the flotation efficiency of mineral particles.

6. Future outlook

The poor flotation of ultrafine particles still remains to be a big challenge confronting academia and industry, which is highlighted by the continuous decrease in particle diameter. Hence, multiphase hydrodynamics simulations, rheological studies of microbubble flotation, and synergistic interaction between microbubbles and reagents have been proposed. On the one hand, most studies are limited to two-phase hydrodynamics simulations, which are quite different from real situations. Therefore, more efforts are needed for the three-phase fluid dynamic simulations and rheological study during microbubble flotation. On the other hand, the synergistic interaction between microbubbles and reagents in enhancing the flotation of ultrafine particles should be studied. In the past few decades, novel collectors and flocculants have been intensively reported to improve the flotation of fine particles. However, little work has been conducted to unveil the synergistic interaction between microbubbles and flotation reagents, which is the key to developing novel flotation reagents and processes.

7. Conclusion

The poor flotation of fine particles is a big problem faced by plants, which has been intensively studied in the past few decades. Microbubbles are effective in improving the flotation of fine particles by promoting the collision and adhesion of particles to bubbles. In this work, the latest advances and progress in the microbubble flotation of fine particles have been systematically reviewed. According to the different ways of producing microbubbles, the preparation methods of microbubbles include PADA, electrolysis, ultrasonic cavitation, photocatalysis, solvent exchange, TDM, Venturi tubes, and microporous membranes. Correspondingly, various flotation columns/machines have been developed for microbubble flotation, such as the Jameson flotation column, pressurized DAF column, electroflotation column, FCSMC, packed flotation column, Yalcin magnetic flotation machine, and magnetic flotation column. In particular, the Jameson flotation column and FCSMC have been widely used in the beneficiation of fine coals, metallic minerals, and nonmetallic minerals, which exhibit better flotation performance than the conventional flotation machine. Mechanisms underpinning nanobubble flotation have been reviewed from the perspective of particle agglomeration, hydrophobicity, and high stability of nanobubbles. In the future, more efforts are still needed to study multiphase hydrodynamics simulation and rheological study and the synergistic interaction between microbubbles and flotation reagents in the flotation of fine particles.

Acknowledgements

This work is funded by the National Natural Science Foundation of China (No. 52004020), Fundamental Research Funds for the Central Universities (No. 00007733), Open Foundation of State Key Laboratory of Mineral Processing (No. BGRIMM-KJSKL-2021-13), High-end Foreign Expert Introduction Program (No. G2022105001L), and State Key Laboratory of Comprehensive Utilization of Low-Grade Refractory Gold Ores, Zijin Mining Group Co., Ltd.

Conflict of Interest

The authors declare that they have no known competing financial interests or personal relationships that could have appeared to influence the work reported in this paper.

References

[1] F.H. Abd El-Rahiem, Recent trends in flotation of fine particles, *J. Min. World Express*, 3(2014), art. No. 63.

[2] P.P. Wang and P.R. Brito-Parada, Dynamics of a particle-laden bubble colliding with an air-liquid interface, *Chem. Eng. J.*, 429(2022), art. No. 132427.

[3] W.P. Du, Research progress on micro-fine particles mineral flotation, *Copper. Eng.*, 2017, No. 2, p. 63.

[4] H.N. Wang, W.Q. Yang, X.K. Yan, L.J. Wang, Y.T. Wang, and H.J. Zhang, Regulation of bubble size in flotation: A review, *J. Environ. Chem. Eng.*, 8(2020), art. No. 104070.

[5] M. Alheshibri, J. Qian, M. Jehannin, and V.S.J. Craig, A history of nanobubbles, *Langmuir*, 32(2016), No. 43, p. 11086.

[6] N. Ahmed and G.J. Jameson, The effect of bubble size on the rate of flotation of fine particles, *Int. J. Miner. Process.*, 14(1985), No. 3, p. 195.

[7] A.S. Reis, A.M. Reis Filho, L.R. Demuner, and M.A.S. Barrozo, Effect of bubble size on the performance flotation of fine particles of a low-grade Brazilian apatite ore, *Powder Technol.*, 356(2019), p. 884.

[8] Q. Zhang, S. Liu, C. Yang, F. Chen, and S. Lu, Bioreactor consisting of pressurized aeration and dissolved air flotation for domestic wastewater treatment, *Sep. Purif. Technol.*, 138(2014), p. 186.

[9] M. Han, Y. Park, J. Lee, and J. Shim, Effect of pressure on bubble size in dissolved air flotation, *Water Supply*, 2(2002), No. 5-6, p. 41.

[10] W.Q. Qin, L.Y. Ren, P.P. Wang, C.R. Yang, and Y.S. Zhang, Efectro-flotation and collision-attachment mechanism of fine cassiterite, *Trans. Nonferrous Met. Soc. China*, 22(2012), No. 4, p. 917.

[11] P.K. Tsave, M. Kostoglou, T.D. Karapantsios, and N.K. Lazaridis, A hybrid device for enhancing flotation of fine particles by combining micro-bubbles with conventional bubbles, *Minerals*, 11(2021), No. 6, art. No. 561.

[12] S. Calgaroto, K.Q. Wilberg, and J. Rubio, On the nanobubbles interfacial properties and future applications in flotation, *Miner. Eng.*, 60(2014), p. 33.

[13] Z.A. Zhou, Z.H. Xu, J.A. Finch, J.H. Masliyah, and R.S. Chow, On the role of cavitation in particle collection in flotation–A critical review. II, *Miner. Eng.*, 22(2009), No. 5, p. 419.

[14] Y. Chen, S.C. Chelgani, X. Bu, and G. Xie, Effect of the ultrasonic standing wave frequency on the attractive mineralization for fine coal particle flotation, *Ultrason. Sonochem.*, 77(2021), art. No. 105682.

[15] Y. Peng, Y. Mao, W. Xia, and Y. Li, Ultrasonic flotation cleaning of high-ash lignite and its mechanism, *Fuel*, 220(2018), p. 558.

[16] M. Kruszelnicki, A. Hassanzadeh, K.J. Legawiec, I. Polowczyk, and P.B. Kowalczuk, Effect of ultrasound pre-treatment on carbonaceous copper-bearing shale flotation, *Ultrason. Sonochem.*, 84(2022), art. No. 105962.

[17] L.O. Filippov, A.S. Matinin, V.D. Samiguin, and I.V. Filippova, Effect of ultrasound on flotation kinetics in the reactor-separator, *J. Phys. Conf. Ser.*, 416(2013), art. No. 012016.

[18] T. Daio, I. Narita, S. Nandy, T. Hisatomi, K. Domen, and K. Suganuma, Direct observation of hydrogen bubble generation on photocatalyst particles by *in situ* electron microscopy, *Chem. Phys. Lett.*, 706(2018), p. 564.

[19] G. Shen, X.H. Zhang, Y. Ming, L.J. Zhang, Y. Zhang, and J. Hu, Photocatalytic induction of nanobubbles on TiO_2 surfaces, *J. Phys. Chem. C*, 112(2008), No. 11, p. 4029.

[20] W.F. Paxton, K.C. Kistler, C.C. Olmeda, *et al.*, Catalytic nanomotors: Autonomous movement of striped nanorods, *J. Am. Chem. Soc.*, 126(2004), No. 41, p. 13424.

[21] M.H. Liu, W.C. Zhao, S. Wang, W. Guo, Y.Z. Tang, and Y.M. Dong, Study on nanobubble generation: Saline solution/water exchange method, *ChemPhysChem*, 14(2013), No. 11, p. 2589.

[22] S.T. Lou, J.X. Gao, X.D. Xiao, *et al.*, Studies of nanobubbles produced at liquid/solid interfaces, *Mater. Charact.*, 48(2002), No. 2-3, p. 211.

[23] W. Guo, H. Shan, M. Guan, L.H. Gao, M.H. Liu, and Y.M. Dong, Investigation on nanobubbles on graphite substrate produced by the water–NaCl solution replacement, *Surf. Sci.*, 606(2012), No. 17-18, p. 1462.

[24] G.Z. Kyzas, A.C. Mitropoulos, and K.A. Matis, From microbubbles to nanobubbles: Effect on flotation, *Processes*, 9(2021), No. 8, art. No. 1287.

[25] M. Wu, S.Y. Yuan, H.Y. Song, and X.B. Li, Micro–nano bubbles production using a swirling-type venturi bubble generator, *Chem. Eng. Process.*, 170(2022), art. No. 108697.

[26] K. Sakamatapan, M. Mesgarpour, O. Mahian, H.S. Ahn, and S. Wongwises, Experimental investigation of the microbubble generation using a venturi-type bubble generator, *Case Stud. Therm. Eng.*, 27(2021), art. No. 101238.

[27] G. Ding, Z. Li, J. Chen, and X. Cai, An investigation on the bubble transportation of a two-stage series venturi bubble generator, *Chem. Eng. Res. Des.*, 174(2021), p. 345.

[28] F.Y. Ma, D.P. Tao, and Y.J. Tao, Effects of nanobubbles in column flotation of Chinese sub-bituminous coal, *Int. J. Coal Prep. Util.*, 42(2022), No. 4, p. 1126.

[29] Y. Xiong and F. Peng, Optimization of cavitation venturi tube design for pico and nano bubbles generation, *Int. J. Min. Sci. Technol.*, 25(2015), No. 4, p. 523.

[30] X. Wang, S. Yuan, J. Liu, Y.M. Zhu, and Y.X. Han, Nanobubble-enhanced flotation of ultrafine molybdenite and the associated mechanism, *J. Mol. Liq.*, 346(2022), art. No. 118312.

[31] M. Wu, H.Y. Song, X. Liang, N. Huang, and X.B. Li, Generation of micro–nano bubbles by self-developed swirl-type micro–nano bubble generator, *Chem. Eng. Process.*, 181(2022), art. No. 109136.

[32] M. Zhao, Y.C. Liu, J.X. Zhang, H. Jiang, and R.Z. Chen, Janus ceramic membranes with asymmetric wettability for high-efficient microbubble aeration, *J. Membr. Sci.*, 671(2023), art. No. 121418.

[33] N. Hornig and U. Fritsching, Liquid dispersion in premix emulsification within porous membrane structures, *J. Membr. Sci.*, 514(2016), p. 574.

[34] X.H. Tao, Y.F. Liu, H. Jiang, and R.Z. Chen, Microbubble generation with shear flow on large-area membrane for fine particle flotation, *Chem. Eng. Process.*, 145(2019), art. No. 107671.

[35] B.Q. Xie, C.J. Zhou, L. Sang, X.D. Ma, and J.S. Zhang, Preparation and characterization of microbubbles with a porous ceramic membrane, *Chem. Eng. Process.*, 159(2021), art. No. 108213.

[36] L.F. Zhou, L.H. Fu, and Q. Zhang, Efficient flotation column for fine particles, *Nonferrous Met.*, 2007, No. 2, p. 55.

[37] P.P. Zhao and Y.J. Cao, Study status of flotation technology and high effective flotation columns for fine mineral, *Met. Mine*, 2011, No. 12, p. 78.

[38] G.C. Wang, X.T. Bai, C.N. Wu, W. Li, K. Liu, and A. Kiani, Recent advances in the beneficiation of ultrafine coal particles, *Fuel Process. Technol.*, 178(2018), p. 104.

[39] S. Li, D.F. Lu, X.H. Chen, *et al.*, Industrial application of a modified pilot-scale Jameson cell for the flotation of spodumene ore in high altitude area, *Powder Technol.*, 320(2017), p. 358.

[40] C. Karagüzel and G. Çobanoğlu, Stage-wise flotation for the removal of colored minerals from feldspathic slimes using laboratory scale Jameson cell, *Sep. Purif. Technol.*, 74(2010), No. 1, p. 100.

[41] A. Gordiychuk, M. Svanera, S. Benini, and P. Poesio, Size distribution and sauter mean diameter of micro bubbles for a Venturi type bubble generator, *Exp. Therm. Fluid Sci.*, 70(2016), p. 51.

[42] M. Uçurum, Influences of Jameson flotation operation variables on the kinetics and recovery of unburned carbon, *Powder Technol.*, 191(2009), No. 3, p. 240.

[43] Y.L. Han, J.B. Zhu, L. Shen, *et al.*, Bubble size distribution characteristics of a jet-stirring coupling flotation device, *Minerals*, 9(2019), No. 6, art. No. 369.

[44] C.Wang, Z.Wang, X.Wei, and X. Li, A numerical studyand flotation experiments of bicyclone column flotation for treating of produced water from ASPflooding, *J. Water Process Eng.*, 32(2019), p. 100972.

[45] X.P. Sun, W.L. Liu, W.S. Wang, S. Chen, and W. Liu, Study on particle size distribution law of air flotation bubble and its influencing factors in coal slime flotation, *Coal Sci. Technol.*,

47(2019), No. 4, p. 205.
[46] Z.Huang,J. Kuang, L. Zhu, W.Yuan, and Z. Zou, Effect ofultrasonication on the separation kinetics of scheelite andcalcite, *Miner. Eng.*,163(2021), art. No.106762.
[47] W. Zhao, J.Z. Qu, Z. Li, Z.Y. Yang, and A.N. Zhou, Influencing factors of electroflotation–electrocoagulation seperation of coal macerals, *Clean Coal Technol.*, 24(2018), No. 1, p. 57.
[48] H.L. Yang, C.Y. Zhu, L. Yi, and X.M. Wu, Research present situation and new progress of flotation column for fine paticles, *Hunan Nonferrous Met.*, 30(2014), No. 5, p. 11.
[49] H.J. Zhang, J.T. Liu, Y.T. Wang, Y.J. Cao, Z.L. Ma, and X.B. Li, Cyclonic-static micro-bubble flotation column, *Miner. Eng.*, 45(2013), p. 1.
[50] X.K. Yan, S.Q. Meng, A. Wang, L.J. Wang, and Y.J. Cao, Hydrodynamics and separation regimes in a cyclonic-static microbubble flotation column, *Asia Pac. J. Chem. Eng.*, 13(2018), No. 3, art. No. e2185.
[51] X.K. Yan, R. Shi, Y.J. Xu, *et al*., Bubble behaviors in a lab-scale cyclonic-static micro-bubble flotation column, *Asia Pac. J. Chem. Eng.*, 11(2016), No. 6, p. 939.
[52] J.D. Miller, Characterization of multiphase fluid flow during air-sparged hydrocyclone flotation by X-ray CT, *Utah University*, Salt Lake City, 1993.
[53] Q. Zhou, Y.J. Cao, X.B. Li, G.P. Niu, and Y.H. Liu, Study on cyclone-static micro-bubble flotation column of scheelite ores, *Nonferrous Met. Miner. Process. Sect.*, 2011, No. 1, p. 39.
[54] X.W. Deng, J.T. Liu, Y.T. Wang, and Y.J. Cao, Velocity distribution of the flow field in the cyclonic zone of cyclone-static micro-bubble flotation column, *Int. J. Min. Sci. Technol.*, 23(2013), No. 1, p. 89.
[55] M.J. Zhao, J.J. Fang, G.D. Li, L. Zhang, and T.M. Zhang, State and application of cyclonic static microbubble flotation column, *Multipurp. Util. Miner. Resour.*, 2016, No. 4, p. 6.
[56] S.A. Idlas, J.A. Fitzpatrick, and J.C. Slattery, Conceptual design of packed flotation columns, *Ind. Eng. Chem. Res.*, 29(1990), No. 6, p. 943.
[57] M. Zhang, T. Li, and G. Wang, A CFD study of the flow characteristics in a packed flotation column: Implications for flotation recovery improvement, *Int. J. Miner. Process.*, 159(2017), p. 60.
[58] B. Wang and H. Jiang, Research and application of flotation column, *Chin. J. Nonferrous Met.*, 31(2021), No. 4, p. 1027.
[59] Z.M. Sun, C.J. Liu, G.C. Yu, and X.G. Yuan, Prediction of distillation column performance by computational mass transfer method, *Chin. J. Chem. Eng.*, 19(2011), No. 5, p. 833.
[60] W.Z. Wang, L.P. Chen, L.B. Zhao, and F.P. Li, Experimental research for application of packed flotation column to reverse flotation of hematite, *Min. Process. Equip.*, 42(2014), No. 2, p. 97.
[61] P.Y. Zhang, S.Z. Jin, L.M. Ou, W.C. Zhang, and Y.T. Zhu, Fine bauxite recovery using a plate-packed flotation column, *Metals*, 10(2020), No. 9, art. No. 1184.
[62] M. Zhang, T.L. Li, S.J. Ma, and G.C. Wang, An experimental study of copper sulfide flotation in a packed cyclonic-static microbubble flotation column, *Sep. Sci. Technol.*, 53(2018), No. 14, p. 2238.
[63] T.S. He and B.C. Chen, Discussion on fine particle flotation equipment, *China Min. Mag.*, 3(1994), No. 4, p. 31.
[64] T. Yalcin, Magnetoflotation: Development and laboratory assessment, *Int. J. Miner. Process.*, 34(1992), No. 1-2, p. 119.
[65] S.X. Shi, L.J. Yang, Z.C. Shen, and S.J. Lu, Research status of fine particle flotation beneficiation methods and equipment, [in] *Proceedings of the Proceedings of the Fifth National Conference on Mining and Dressing Technology Progress*, Hohhot, 2006, p. 121.
[66] Z.C. Shen, D. Chen, S.X. Shi, S.J. Lu, and L. Meng, Development of BGRIMM flotation column technology, *Nonferrous Met. Miner. Process. Sect.*, 2006, No. 6, p. 33.
[67] R.D. Deng, Q.J. Liu, T. Hu, and F.H. Ye, Concentration of high-sulfur copper ore using a three-product magnetic flotation column, *Min. Metall. Explor.*, 30(2013), No. 2, p. 122.
[68] Y. Liao, Z. Ma, and Y. Cao, Improving reverse flotation of magnetite ore using pulse magnetic field, *Miner. Eng.*, 138(2019), p. 108.
[69] X.X. Tao, Y.J. Cao, J. Liu, K.Y. Shi, J.Y. Liu, and M.M. Fan, Studies on characteristics and flotation of a hard-to-float high-ash fine coal, *Procedia Earth Planet. Sci.*, 1(2009), No. 1, p. 799.
[70] G.J. Jameson, New directions in flotation machine design, *Miner. Eng.*, 23(2010), No. 11-13, p. 835.
[71] G.Q. Xu, Y.R. Chen, X.N. Bu, X.S. Dong, G.Y. Xie, and Y.J. Sun, Separation performance of mechanical flotation cell and cyclonic microbubble flotation column: In terms of the beneficiation of high-ash coal fines, *Energy Sources A*, 42(2020), No. 23, p. 2845.
[72] M.M. Fan, D. Tao, R. Honaker, and Z.F. Luo, Nanobubble generation and its applications in froth flotation (Part IV): Mechanical cells and specially designed column flotation of coal, *Min. Sci. Technol. China*, 20(2010), No. 5, p. 641.
[73] C.W. Li, M. Xu, Y.W. Xing, H.J. Zhang, and U.A. Peuker, Efficient separation of fine coal assisted by surface nanobubbles, *Sep. Purif. Technol.*, 249(2020), art. No. 117163.
[74] A. Sobhy and D.P. Tao, Nanobubble column flotation of fine coal particles and associated fundamentals, *Int. J. Miner. Process.*, 124(2013), p. 109.
[75] Z. Zhang, L. Ren, and Y. Zhang, Role of nanobubbles in the flotation of fine rutile particles, *Miner. Eng.*, 172(2021), art. No. 107140.
[76] D. Tao, Z. Wu, and A. Sobhy, Investigation of nanobubble enhanced reverse anionic flotation of hematite and associated mechanisms, *Powder Technol.*, 379(2021), p. 12.
[77] G.X. Fan, J.T. Liu, Y.J. Cao, and T. Huo, Optimization of fine ilmenite flotation performed in a cyclonic-static micro-bubble flotation column, *Physicochem. Probl. Miner. Pro.*, 50(2014), No. 2, p. 823.
[78] R. Ahmadi, D.A. Khodadadi, M. Abdollahy, and M.M. Fan, Nano–microbubble flotation of fine and ultrafine chalcopyrite particles, *Int. J. Min. Sci. Technol.*, 24(2014), No. 4, p. 559.
[79] R. Ahmadi and A. Darban, Modeling and optimization of nano-bubble generation process using response surface methodology, *Int. J. Nanosci. Nanotechnol.*, 9(2013), p. 151.
[80] Y. Cheng, Y.S. Song, B. Li, and Q.Q. Wang, Experimental research on the column flotation of micro-fine pyrite particles, *Met. Mine*, 2009, No. 6, p. 64.
[81] V. Chipakwe, A. Sand, and S.C. Chelgani, Nanobubble assisted flotation separation of complex Pb–Cu–Zn sulfide ore-Assessment of process readiness, *Sep. Sci. Technol.*, 57(2022), No. 8, p. 1351.
[82] Y.C. Cao, G.Y. Huang, L.Y. Yang, S.W. Liu, and Q.X. Deng, Experimental study on flotation of some copper ore by using crimm flotation cell, *Hunan Nonferrous Met.*, 33(2017), No. 4, p. 11.
[83] P.G. Wei, L.Y. Ren, Y.M. Zhang, and S.X. Bao, Influence of microbubble on fine wolframite flotation, *Minerals*, 11(2021),

No. 10, art. No. 1079.

[84] J.R. Zhang, *Dispersion Behavior and Mechanism of Micro-fine Fluorite and Quartz* [Dissertation], Inner Mongolia University of Science and Technology, Inner Mongolia Autonomous Region, 2021.

[85] Y.T. Wang, The application and development of microbubble column flotation technology in China, *Adv. Mater. Res.*, 136(2010), p. 194.

[86] W.S. Chen, J.T. Liu, X.B. Li, Y.J. Cao, and Y.T. Wang, Analysis of factors influencing fluorite flotation by cyclonic static micro-bubble flotation column, *Met. Mine*, 2008, No. 5, p. 100.

[87] S. Farrokhpay, I. Filippova, L. Filippov, A. Picarra, N. Rulyov, and D. Fornasiero, Flotation of fine particles in the presence of combined microbubbles and conventional bubbles, *Miner. Eng.*, 155(2020), art. No. 106439.

[88] S. Calgaroto, A. Azevedo, and J. Rubio, Flotation of quartz particles assisted by nanobubbles, *Int. J. Miner. Process.*, 137(2015), p. 64.

[89] A.F. Rosa and J. Rubio, On the role of nanobubbles in particle–bubble adhesion for the flotation of quartz and apatitic minerals, *Miner. Eng.*, 127(2018), p. 178.

[90] X.N. Bu, G.Y. Xie, Y.L. Peng, and Y.R. Chen, Corrigendum to "Kinetic modeling and optimization of flotation process in a cyclonic microbubble flotation column using composite central design methodology", *Int. J. Miner. Process.*, 157(2016), p. 175.

[91] F. Ma, D. Tao, Y. Tao, and S. Liu, An innovative flake graphite upgrading process based on HPGR, stirred grinding mill, and nanobubble column flotation, *Int. J. Min. Sci. Technol.*, 31(2021), No. 6, p. 1063.

[92] W. Liu, Application of Jameson flotation machine in coking coal preparation plant, *Coal Chem. Ind.*, 41(2018), No. 3, p. 129.

[93] Y. Liu, Y.J. Cao, G. Huang, J. Dong, and W.J. Zou, Semi-industrial test of a gold ore slime separation by cyclonic-static micro-bubble flotation column, *Met. Mine*, 2012, No. 3, p. 82.

[94] Y.F. Zhu, J.T. Liu, Y.J. Cao, and Y.T. Wang, Experimental study on copper cleaning by using cyclonic-static microbubble flotation column, *China Mine Eng.*, 40(2011), No. 3, p. 13.

[95] W.Z. Wang, M.M. Han, and C.G. Yang, Applied research of cyclonic-static micro-bubble flotation column on the microfine hematite flotation, *Adv. Mater. Res.*, 641(2013), p. 242.

[96] G.S. Zheng, J.T. Liu, L. Li, Z.J. Zhang, and H.W. Qian, Reverse flotation of the iron concentrate from magnetic separation by cyclonic static micro-bubble flotation column, *Met. Mine*, 2008, No. 8, p. 40.

[97] H.J. Qin, H.J. Zhang, C. He, X.T. Gao, and X. Ma, Study on the recovery of molybdenum in molybdenum cleaner tailings using cyclonic-static microbubble flotation column, *China Molybdenum Ind.*, 40(2016), No. 4, p. 6.

[98] T.T. Zhang, Y.L. Peng, G.Y. Xie, Y.R. Chen, and X.N. Bu, Experiment of flotation of microcrystalline graphite by cyclonic micro-bubble flotation column and flotator, *Non Met. Mines*, 40(2017), No. 1, p. 7.

[99] L.M. Ou, L.J. Wang, Q.M. Feng, L. Wan, and J.S. Ye, Beneficiation of middle-low grade bauxite with micro-bubble flotation column, *Min. Metall. Eng.*, 31(2011), No. 3, p. 40.

[100] R.C. Santana, J.A. Ribeiro, M.A. Santos, A.S. Reis, C.H. Ataíde, and M.A.S. Barrozo, Flotation of fine apatitic ore using microbubbles, *Sep. Purif. Technol.*, 98(2012), p. 402.

[101] D.P. Tao, M.M. Fan, Z.X. Wu, X.Y. Zhang, Q.S. Wang, and Z.K. Li, Investigation of effects of nanobubbles on phosphate ore flotation, *Int. J. Georesources Environ.*, 4(2018), No. 3, p. 133.

[102] C. Li and H. Zhang, Surface nanobubbles and their roles in flotation of fine particles-A review, *J. Ind. Eng. Chem.*, 106(2022), p. 37.

[103] M. Buchmann, G. Öktem, M. Rudolph, and K.G.V. den Boogaart, Proposition of a bubble-particle attachment model based on DLVO van der Waals and electric double layer interactions for froth flotation modelling, *Physicochem. Probl. Miner. Pro.*, 58(2022), No. 5.

[104] P. Knüpfer, L. Ditscherlein, and U.A. Peuker, Nanobubble enhanced agglomeration of hydrophobic powders, *Colloids Surf. A*, 530(2017), p. 117.

[105] M.A. Hampton and A.V. Nguyen, Nanobubbles and the nanobubble bridging capillary force, *Adv. Colloid Interface Sci.*, 154(2010), No. 1-2, p. 30.

[106] N.N. Rulyov, Combined microflotation of fine minerals: Theory and experiment, *Miner. Process. Extr. Metall.*, 125(2016), No. 2, p. 81.

[107] L. Ditscherlein, P. Knüpfer, and U.A. Peuker, The influence of nanobubbles on the interaction forces between alumina particles and ceramic foam filters, *Powder Technol.*, 357(2019), p. 408.

[108] C.W. Li, K.K. Zhen, Y.N. Hao, and H.J. Zhang, Effect of dissolved gases in natural water on the flotation behavior of coal, *Fuel*, 233(2018), p. 604.

[109] T.B. Zhang and Q. Zhang, Research of nanobubbles enhanced reverse anionic flotation of a mid-low grade phosphate ore, *Physicochem. Probl. Miner. Pro.*, 58(2022).

[110] E. Bird and Z. Liang, Nanobubble capillary force between parallel plates, *Phys. Fluids*, 34(2022), No. 1, art. No. 013301.

[111] F.F. Zhang, L.J. Sun, H.C. Yang, *et al*., Recent advances for understanding the role of nanobubbles in particles flotation, *Adv. Colloid Interface Sci.*, 291(2021), art. No. 102403.

[112] W.G. Zhou, L.M. Ou, Q. Shi, Q.M. Feng, and H. Chen, Different flotation performance of ultrafine scheelite under two hydrodynamic cavitation modes, *Minerals*, 8(2018), No. 7, art. No. 264.

[113] L.Y. Ren, W.N. Zeng, Z.Y. Zhang, and P.G. Wei, Visualization of effect of micro–nano bubbles on aggregation of fine cassiterite, *Chin. J. Nonferrous Met.*, 32(2022), No. 5, p. 1479.

[114] H. An, G. Liu, and V.S. Craig, Wetting of nanophases: Nanobubbles, nanodroplets and micropancakes on hydrophobic surfaces, *Adv. Colloid Interface Sci.*, 222(2015), p. 9.

[115] D.J. Johnson, S.A. Al Malek, B.A.M. Al-Rashdi, and N. Hilal, Atomic force microscopy of nanofiltration membranes: Effect of imaging mode and environment, *J. Membr. Sci.*, 389(2012), p. 486.

[116] V.S.J. Craig, Very small bubbles at surfaces-the nanobubble puzzle, *Soft Matter*, 7(2011), No. 1, p. 40.

[117] F.Y. Ma, P. Zhang, and D.P. Tao, Surface nanobubble characterization and its enhancement mechanisms for fine-particle flotation: A review, *Int. J. Miner. Metall. Mater.*, 29(2022), No. 4, p. 727.

[118] Y.W. Liu and X.R. Zhang, A review of recent theoretical and computational studies on pinned surface nanobubbles, *Chin. Phys. B*, 27(2018), No. 1, art. No. 014401.

[119] D. Tao, Recent advances in fundamentals and applications of nanobubble enhanced froth flotation: A review, *Miner. Eng.*,

183(2022), art. No. 107554.
[120] S. Ljunggren and J.C. Eriksson, The lifetime of a colloid-sized gas bubble in water and the cause of the hydrophobic attraction, *Colloids Surf. A*, 129-130(1997), p. 151.
[121] N. Ishida, T. Inoue, M. Miyahara, and K. Higashitani, Nano bubbles on a hydrophobic surface in water observed by tapping-mode atomic force microscopy, *Langmuir*, 16(2000), No. 16, p. 6377.
[122] A. Azevedo, R. Etchepare, S. Calgaroto, and J. Rubio, Aqueous dispersions of nanobubbles: Generation, properties and features, *Miner. Eng.*, No.(2016), p. 29.
[123] W.A. Ducker, Contact angle and stability of interfacial nanobubbles, *Langmuir*, 25(2009), No. 16, p. 8907.
[124] N.D. Petsev, M.S. Shell, and L.G. Leal, Dynamic equilibrium explanation for nanobubbles' unusual temperature and saturation dependence, *Phys. Rev. E*, 88(2013), No. 1, art. No. 010402.
[125] H. Peng, G.R. Birkett, and A.V. Nguyen, Origin of interfacial nanoscopic gaseous domains and formation of dense gas layer at hydrophobic solid–water interface, *Langmuir*, 29(2013), No. 49, p. 15266.
[126] H. Peng, G.R. Birkett, and A.V. Nguyen, Progress on the surface nanobubble story: What is in the bubble? Why does it exist? *Adv. Colloid Interface Sci.*, 222(2015), p. 573.
[127] P.E. Theodorakis and Z.Z. Che, Surface nanobubbles: Theory, simulation, and experiment. A review, *Adv. Colloid Interface Sci.*, 272(2019), art. No. 101995.
[128] J.R.T. Seddon, H.J.W. Zandvliet, and D. Lohse, Knudsen gas provides nanobubble stability, *Phys. Rev. Lett.*, 107(2011), No. 11, art. No. 116101.